

TWO-STEP COLOR-POLARIZATION DEMOSAICKING NETWORK

Vy Nguyen, Masayuki Tanaka, Yusuke Monno, and Masatoshi Okutomi

Tokyo Institute of Technology, Tokyo, Japan

ABSTRACT

Polarization information of light in a scene is valuable for various image processing and computer vision tasks. A division-of-focal-plane polarimeter is a promising approach to capture the polarization images of different orientations in one shot, while it requires color-polarization demosaicking. In this paper, we propose a two-step color-polarization demosaicking network (TCPDNet), which consists of two sub-tasks of color demosaicking and polarization demosaicking. We also introduce a reconstruction loss in the YCbCr color space to improve the performance of TCPDNet. Experimental comparisons demonstrate that TCPDNet outperforms existing methods in terms of the image quality of polarization images and the accuracy of Stokes parameters.

Index Terms— Color-polarization filter array, color demosaicking, polarization demosaicking, deep learning

1. INTRODUCTION

Polarization information of light in a scene can be helpful in various image processing and computer vision tasks such as transparent object segmentation [1], 3D reconstruction [2], and specular removal [3]. A polarization image can be obtained by placing a polarizer in front of the camera lens, where the images of different polarization orientations of the same scene can be obtained by rotating the polarizer. Four polarization images of 0° , 45° , 90° , and 135° are typically captured to robustly infer necessary polarization information, e.g., Stokes parameters, the angle of polarization (AoP), and the degree of polarization (DoP) [4].

There are two popular polarization image acquisition approaches [5]: a division-of-time polarimeter and a division-of-focal-plane polarimeter. In the division-of-time polarimeter, a linear polarizer in front of the camera lens is sequentially rotated in time to obtain different polarization states of a pixel. However, the division-of-time polarimeter is only applicable to static scenes where no camera and object movement exists. In the division-of-focal-plane polarimeter, a micro-polarizer

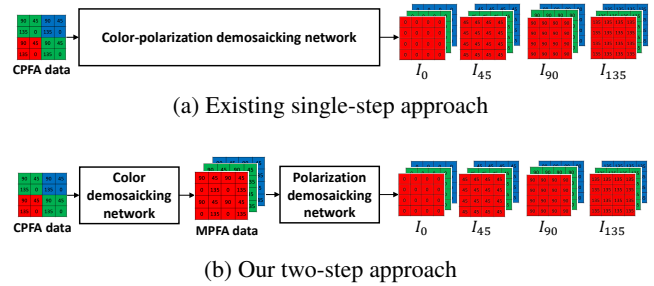


Fig. 1: Two network-based approaches for color-polarization demosaicking: (a) Existing single-step approach and (b) our two-step approach, which consists of color demosaicking and polarization demosaicking.

array is used to capture different polarization orientations as a mosaic pattern at once. Each pixel of the captured mosaic pattern only contains the information of one polarization orientation. The division-of-focal-plane polarimeter can be applied to dynamic scenes but it requires a demosaicking process, which is an interpolation process of missing pixel values. The demosaicking process strongly affects the image quality.

In this paper, we focus on color-polarization filter array (CPFA) demosaicking for a color division-of-focal-plane polarimeter, such as a Sony sensor [6]. Typically, the input of the CPFA demosaicking is 1-channel CPFA raw data and the output is 12-channel full-color-polarization images, as shown in Fig. 1. Each pixel of the input 1-channel CPFA raw data contains the intensity of one polarization orientation and one color channel. The output 12-channel full-color-polarization images are a set of RGB and four polarization images with the angles of 0° , 45° , 90° , and 135° . The CPFA demosaicking is more challenging than color filter array (CFA) demosaicking and monochrome polarization filter array (MPFA) demosaicking, because the sampling density of each color-polarization component in the CPFA raw data is very low.

There are two typical approaches of the CPFA demosaicking problem: An interpolation-based approach [7, 8] and a learning-based approach [9, 10, 11]. The interpolation-based approach is simple, but the performance is usually limited. Because the learning-based approach with a deep neural network has great potential to obtain high performance, we adopt a network-based approach in this paper.

In the literature, there are two representative learning-

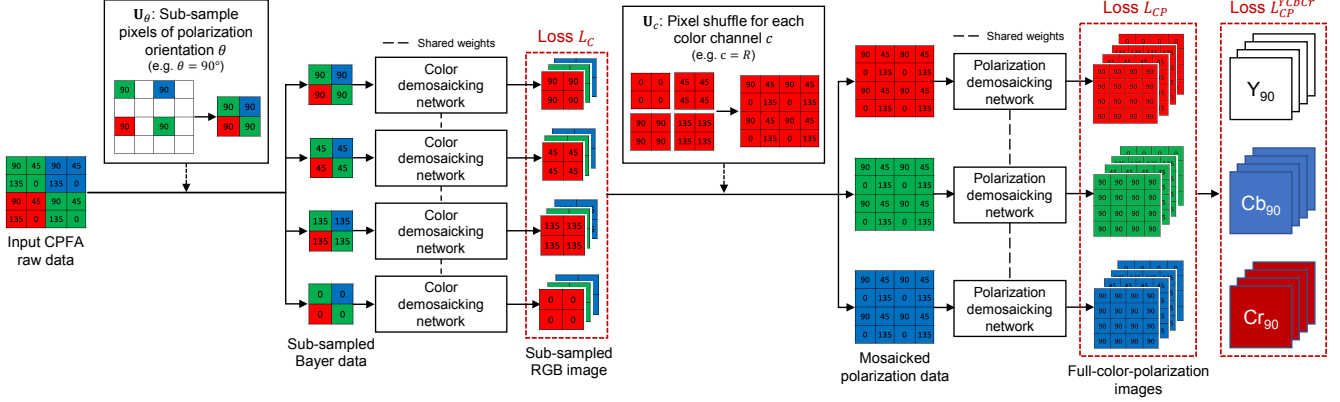


Fig. 2: The overall pipeline of our Two-step Color-Polarization Demosaicking Network (TCPDNet).

based CPFA demosaicking methods: CPDNet [10] and CPD-CNN [11]. CPDNet is an end-to-end network which directly processes the CPFA raw data [10]. CPDCNN is a two-branch network which includes the sub-networks to exploit inter-channel correlations and high-frequency information [11]. Both of them process the color and the polarization information in an intertwined manner.

In this work, we propose a two-step color-polarization demosaicking network (TCPDNet). The network architecture of TCPDNet is inspired by Morimatsu’s interpolation-based CPFA demosaicking method [7, 8]. Our method consists of two well-studied sub-tasks: color demosaicking [12, 13] and polarization demosaicking [14, 15, 16], as shown in Fig. 1(b). In each sub-task, demosaicking network parameters are shared across different kinds of input mosaicked data. We consider that even if the input mosaicked data differ in polarization orientations (for the color demosaicking task) or color channels (for the polarization demosaicking task), their inter-channel correlations should be the same. For example, the color demosaicking networks for 0° of Bayer CFA mosaicked data and 90° of Bayer CFA mosaicked data share the same parameters because their RGB correlations should be the same regardless of the polarization orientations. We further improve the performance of TCPDNet by introducing a reconstruction loss in the YCbCr color space. Using the loss function in the YCbCr color space, we expect the demosaicking networks to learn the inter-channel correlations effectively. Experimental results show that our TCPDNet outperforms existing methods by a large margin both quantitatively and qualitatively on Tokyo Tech dataset [7, 8] and CPDNet dataset [10].

2. PROPOSED METHOD

2.1. Network architecture

Proposed TCPDNet consists of two sub-networks: color demosaicking network and polarization demosaicking network.

This is inspired by the work of Morimatsu et al. [7, 8], which proposes a two-step interpolation-based color-polarization demosaicking method. Figure 2 shows the overall pipeline of our proposed method. The input CPFA raw data are firstly re-arranged into four sub-sampled Bayer mosaicked data. The sub-sampled Bayer mosaicked data has half size of input raw data in height and in width. The color demosaicking networks then demosaick these four sub-sampled Bayer mosaicked data to generate four sub-sampled RGB images, where the weights of the color demosaicking networks are shared. Then, three mosaicked polarization data are generated by the same manner as the pixel shuffle operation [17]. Then, polarization demosaicking networks demosaick those three mosaicked polarization data to generate full-RGB-polarization images which form the output 12-channel data, where the weights of the polarization demosaicking networks are also shared.

Color demosaicking network and polarization demosaicking network have the same demosaicking strategy. Given the input 1-channel mosaicked data, we first interpolate the mosaicked data by bilinear interpolation and then refine the interpolated image by CNN, for which we adopt a high-performance network of U-net [18] with the skip connection, though any kind of CNN architectures can be applied.

2.2. Loss function

We evaluate reconstruction losses with two kinds of images: sub-sampled RGB images and full-color-polarization images, in comparison with the ground-truth data. We refer to the reconstruction losses of the sub-sampled RGB images and the full-color-polarization images as L_C and L_{CP} , respectively, as described in Fig. 2.

In this paper, we use the L1-norm for the reconstruction losses. We also introduce L_{CP}^{YCbCr} , which is the reconstruction loss of the full-color-polarization images in the YCbCr color space, as shown in Fig. 2. The backpropagation training with the L_{CP} loss in the RGB color space updates the weights of the polarization demosaicking network in a channel-by-channel

manner, while the training with the L_{CP}^{YCbCr} loss in the YCbCr color space is expected to take account of inter-channel correlations.

Let \mathbf{X} be the input CPFA raw data, and \mathbf{Z} be the ground-truth 12-channel full-color-polarization data. Let H be the input height and W be the input width. Let \mathbf{g}_Φ be the color demosaicking network with the parameter Φ and \mathbf{h}_Ψ be the polarization demosaicking network with the parameter Ψ . Let Θ be $\{0^\circ, 45^\circ, 90^\circ, 135^\circ\}$ which is a set of polarization orientations.

For the color demosaicking network, let \mathbf{U}_θ ($\theta \in \Theta$) be the process which sub-samples pixels of polarization orientation θ from \mathbf{X} to form 1-channel sub-sampled Bayer CFA mosaicked data, let \mathbf{V}_θ be the process which extracts sub-sampled RGB image for polarization angle θ from the full-color-polarization images \mathbf{Z} . The reconstruction loss of the sub-sampled RGB images can be expressed as

$$L_C(\Phi; \mathbf{X}, \mathbf{Z}) = \frac{1}{3HW} \sum_{\theta \in \Theta} \|\mathbf{g}_\Phi(\mathbf{U}_\theta(\mathbf{X})) - \mathbf{V}_\theta(\mathbf{Z})\|_1. \quad (1)$$

For the polarization demosaicking network, let $\mathbf{Y}(\mathbf{X}; \Phi) = \{\mathbf{g}_\Phi(\mathbf{U}_\theta(\mathbf{X})) | \theta \in \Theta\}$ be a set of the outputs of the color demosaicking network. Let \mathbf{U}_c ($c \in \{R, G, B\}$) be the pixel shuffle operation for c -channel of $\mathbf{Y}(\mathbf{X}; \Phi)$. Let \mathbf{V}_c be the process to extract c -channel from the full-color-polarization images \mathbf{Z} . The reconstruction loss of the full-color-polarization images can be expressed as

$$L_{CP}(\Phi, \Psi; \mathbf{X}, \mathbf{Z}) = \frac{1}{12HW} \sum_{c \in \{R, G, B\}} \|\mathbf{h}_\Psi(\mathbf{U}_c(\mathbf{Y}(\mathbf{X}; \Phi))) - \mathbf{V}_c(\mathbf{Z})\|_1. \quad (2)$$

The reconstruction loss in Eq. 2 is evaluated in the RGB color space. We then introduce the reconstruction loss in the YCbCr color space. Let \mathbf{A} be the function which converts 12-channel full-color-polarization images from the RGB color space to the YCbCr color space and let Con_c be the operation that concatenates each-channel result to form full-color-polarization images. The reconstruction loss in the YCbCr color space can be expressed as

$$L_{CP}^{YCbCr}(\Phi, \Psi; \mathbf{X}, \mathbf{Z}) = \frac{1}{12HW} \|\mathbf{A}(Con_c(\mathbf{h}_\Psi(\mathbf{U}_c(\mathbf{Y}(\mathbf{X}; \Phi)))) - \mathbf{A}(\mathbf{Z})\|_1. \quad (3)$$

Then, our proposed loss function can be expressed by combining two reconstruction losses as

$$L = L_C + \alpha L_{CP}^{YCbCr}, \quad (4)$$

Table 1: Ablation study on different loss combinations of TCPDNet and the single-step network on Tokyo Tech dataset.

Method	Loss	CPSNR		Angle error
		S_0	DoP	AoP
Single-step	L_{CP}	44.72	37.03	14.30
	L_{CP}^{YCbCr}	44.58	36.71	14.63
TCPDNet	$L_C + 4L_{CP}$	44.59	38.74	12.70
	$L_C + 4L_{CP}^{YCbCr}$	44.91	38.74	12.65

where α is a hyperparameter.

In this paper, we experientially set 4 for α . The experimental results later show that the loss combination $L_C + 4L_{CP}^{YCbCr}$ significantly outperforms the loss combination $L_C + 4L_{CP}$, which proves the effectiveness of L_{CP}^{YCbCr} over L_{CP} .

3. EXPERIMENTAL RESULTS

3.1. Datasets and metrics

We evaluated the proposed network with two publicly available datasets: Tokyo Tech dataset [7] and CPDNet dataset [10]. Due to the page limitation, we only show the results on Tokyo Tech dataset in this paper. Additional results on Tokyo Tech and CPDNet datasets can be seen as a supplemental material in our project page¹. In those two datasets, the ground-truth 12-channel full-color-polarization images were taken by the division-of-time polarimeter approach. Then, the CPFA raw data were synthesized with the corresponding CPFA pattern. We quantitatively evaluated with Color Peak Signal-to-Noise Ratio (CPSNR) and the angle error of AoP following related works of [7, 8].

Tokyo Tech dataset includes 40 scenes of 1024×768 resolution. The evaluations in this work were conducted on our splits: 30 scenes for the training set, two scenes for the validation set, and eight scenes for the testing set.

3.2. Training details

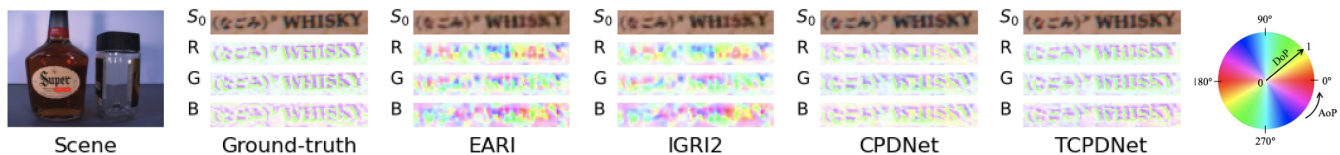
We trained the networks with 64×64 sized patches cropped from the full size of the training image, while we tested with the full size of the test image. For the training batch generation, first, we randomly sampled six different images. Then, four image patches were cropped from each sampled image. Therefore, one training batch for updating the network weight consists of 24 image patches. We used Adam optimizer [19] with a fixed learning rate of 10^{-4} through the training. Each model was trained with 200,000 iterations. Our code is available at our project page (see footnote 1).

For data augmentation, we applied the random rotation of 0° , 90° , 180° and 270° on the 12-channel ground-truth

¹<http://www.ok.sc.e.titech.ac.jp/res/PolarDem/TCPDNet.html>

Table 2: Performance comparison on Tokyo Tech dataset.

Method	CPSNR								Angle error
	I_0	I_{45}	I_{90}	I_{135}	S_0	S_1	S_2	DoP	AoP
Bilinear interpolation	34.64	34.27	35.19	34.46	36.01	42.05	39.93	30.33	23.70
EARI [7]	38.33	37.58	39.00	37.77	39.81	45.47	42.82	32.95	20.54
IGRI2 [8]	38.40	37.59	39.07	37.78	39.60	46.38	43.05	33.17	20.05
CPDNet (original) [10]	23.02	24.26	24.33	24.43	24.64	32.35	38.96	24.85	50.42
CPDNet (re-trained) [10]	28.01	27.81	28.10	27.81	28.23	45.23	41.84	31.24	32.32
TCPDNet (Ours)	43.73	43.16	44.46	43.31	44.91	52.82	48.86	38.74	12.65

**Fig. 3:** Qualitative comparison between our proposed TCPDNet and existing methods. The scene is from Tokyo Tech dataset.

full-color-polarization images before CPFA raw data synthesis. Applying clockwise 90° rotation on the polarization image is equivalent to rotating the camera by clockwise 90° around its Z-axis, which results in the change of AoP. For this case, every pixel in the AoP image should be subtracted by 90° [1]. We took this AoP change into account by re-arranging the order of polarization channels of the 12-channel ground-truth full-color-polarization images from $[I_0, I_{45}, I_{90}, I_{135}]$ to $[I_{90}, I_{135}, I_0, I_{45}]$. Similar polarization channel re-arrangements were also applied for clockwise 180° rotation and clockwise 270° rotation.

3.3. Ablation study

We evaluated two network architectures and two losses in different color spaces. We compared the proposed TCPDNet with the single-step color-polarization network. We also compared the L_{CP} loss in the RGB color space and the L_{CP}^{YCbCr} loss in the YCbCr color space. Our ablation study was conducted with Tokyo Tech dataset.

From Table 1, we find that the L_{CP}^{YCbCr} loss does not contribute to the improvement of the single-step network, but it greatly improves the performance of TCPDNet. This is expected because the single-step network jointly generates the full-color-polarization images originally, while the proposed TCPDNet generates those per monochrome. Thus, the L_{CP}^{YCbCr} loss plays an important role in exploiting the inter-channel correlations in our TCPDNet to boost the performance.

3.4. Comparison with existing methods

We compared our proposed TCPDNet trained with the loss combination $L_C + 4L_{CP}^{YCbCr}$ against other existing methods on Tokyo Tech dataset. We compared with five algorithms; bilinear interpolation, EARI [7], IGRI2 [8], CPDNet [10] (origi-

nal), and CPDNet [10] (re-trained). The weight of CPDNet (original) is provided by the authors of [10], while we re-trained CPDNet (re-trained) with Tokyo Tech dataset. For the learning-based methods, each model was trained five times and averaged metric values were evaluated.

Table 2 shows the quantitative comparisons with Tokyo Tech dataset, where a higher CPSNR is better and a lower angle error is better. We evaluated four color-polarization images (I_0, I_{45}, I_{90} , and I_{135}), three Stokes parameters (S_0, S_1 , and S_2), DoP, and AoP. From Table 2, we can find that the proposed TCPDNet clearly outperforms the other existing methods by a large margin.

We conducted the qualitative comparison on S_0 and the visualizations of DoP and AoP. Figure 3 visualizes the results of different methods for a scene from Tokyo Tech dataset, where we visualize AoP-DoP with the same manner as [7, 8]. Our proposed TCPDNet can produce better results with clearer edges and fewer artifacts. On the other hand, we can observe obvious color artifacts in S_0 estimated by existing methods, especially on the character "S". Regarding the results of the AoP-DoP visualization, EARI and IGRI2 hardly preserve the edge information. The re-trained CPDNet generally provides better results but not as close to the ground truth as TCPDNet.

4. CONCLUSION

In this work, we have proposed a two-step color-polarization demosaicking network, referred as TCPDNet. This network comprises of two sub-networks: color demosaicking network and polarization demosaicking network. We have also introduced the reconstruction loss in the YCbCr color space for the improvement of TCPDNet. Our proposed TCPDNet quantitatively and qualitatively outperforms existing methods by

a significant margin. Comparing to existing methods, our TCPDNet is the best in preserving the edge information with the least color artifacts.

5. REFERENCES

- [1] Agastya Kalra, Vage Taamazyan, Supreeth Krishna Rao, Kartik Venkataraman, Ramesh Raskar, and Achuta Kadambi, “Deep polarization cues for transparent object segmentation,” *Proc. of IEEE/CVF Conf. on Computer Vision and Pattern Recognition (CVPR)*, pp. 8602–8611, 2020.
- [2] Jinyu Zhao, Yusuke Monno, and Masatoshi Okutomi, “Polarimetric multi-view inverse rendering,” *Proc. of European Conf. on Computer Vision (ECCV)*, pp. 85–102, 2020.
- [3] Laurent Valentin Jospin, Gilles Baechler, and Adam Schofield, “Embedded polarizing filters to separate diffuse and specular reflection,” *Proc. of Asian Conf. on Computer Vision (ACCV)*, pp. 3–18, 2018.
- [4] Cong Phuoc Huynh, Antonio Robles-Kelly, and Edwin R Hancock, “Shape and refractive index from single-view spectro-polarimetric images,” *Int. Journal of Computer Vision*, vol. 101, no. 1, pp. 64–94, 2013.
- [5] J Scott Tyo, Dennis L Goldstein, David B Chenault, and Joseph A Shaw, “Review of passive imaging polarimetry for remote sensing applications,” *Applied Optics*, vol. 45, no. 22, pp. 5453–5469, 2006.
- [6] Yasushi Maruyama, Takashi Terada, Tomohiro Yamazaki, Yusuke Uesaka, Motoaki Nakamura, Yoshihisa Matoba, Kenta Komori, Yoshiyuki Ohba, Shinichi Arakawa, Yasutaka Hirasawa, Yuhiko Kondo, Jun Murayama, Kentaro Akiyama, Yusuke Oike, Shuzo Sato, and Takayuki Ezaki, “3.2-MP back-illuminated polarization image sensor with four-directional air-gap wire grid and 2.5- μm pixels,” *IEEE Trans. on Electron Devices*, vol. 65, no. 6, pp. 2544–2551, 2018.
- [7] Miki Morimatsu, Yusuke Monno, Masayuki Tanaka, and Masatoshi Okutomi, “Monochrome and color polarization demosaicking using edge-aware residual interpolation,” *Proc. of IEEE Int. Conf. on Image Processing (ICIP)*, pp. 2571–2575, 2020.
- [8] Miki Morimatsu, Yusuke Monno, Masayuki Tanaka, and Masatoshi Okutomi, “Monochrome and color polarization demosaicking based on intensity-guided residual interpolation,” *IEEE Sensors Journal*, vol. 21, no. 23, pp. 26985–26996, 2021.
- [9] Sijia Wen, Yinqiang Zheng, and Feng Lu, “A sparse representation based joint demosaicing method for single-chip polarized color sensor,” *IEEE Trans. on Image Processing*, vol. 30, pp. 4171–4182, 2021.
- [10] Sijia Wen, Yinqiang Zheng, Feng Lu, and Qiping Zhao, “Convolutional demosaicing network for joint chromatic and polarimetric imagery,” *Optics Letters*, vol. 44, no. 22, pp. 5646–5649, 2019.
- [11] Yuanyuan Sun, Junchao Zhang, and Rongguang Liang, “Color polarization demosaicking by a convolutional neural network,” *Optics Letters*, vol. 46, no. 17, pp. 4338–4341, 2021.
- [12] Daisuke Kiku, Yusuke Monno, Masayuki Tanaka, and Masatoshi Okutomi, “Beyond color difference: Residual interpolation for color image demosaicking,” *IEEE Trans. on Image Processing*, vol. 25, no. 3, pp. 1288–1300, 2016.
- [13] Yusuke Monno, Daisuke Kiku, Masayuki Tanaka, and Masatoshi Okutomi, “Adaptive residual interpolation for color and multispectral image demosaicking,” *Sensors*, vol. 17, no. 12, pp. 2787, 2017.
- [14] Sofiane Mihoubi, Pierre-Jean Lapray, and Laurent Bigué, “Survey of demosaicking methods for polarization filter array images,” *Sensors*, vol. 18, no. 11, pp. 3688, 2018.
- [15] Ashfaq Ahmed, Xiaojin Zhao, Jintao Chang, Hui Ma, Viktor Gruev, and Amine Bermak, “Four-directional adaptive residual interpolation technique for DoFP polarimeters with different micro-polarizer patterns,” *IEEE Sensors Journal*, vol. 18, no. 19, pp. 7990–7997, 2018.
- [16] Tuochi Jiang, Desheng Wen, Zongxi Song, Weikang Zhang, Zhixin Li, Xin Wei, and Gang Liu, “Minimized laplacian residual interpolation for DoFP polarization image demosaicking,” *Applied Optics*, vol. 58, no. 27, pp. 7367–7374, 2019.
- [17] Wenzhe Shi, Jose Caballero, Ferenc Huszár, Johannes Totz, Andrew P Aitken, Rob Bishop, Daniel Rueckert, and Zehan Wang, “Real-time single image and video super-resolution using an efficient sub-pixel convolutional neural network,” *Proc. of IEEE Conf. on Computer Vision and Pattern Recognition (CVPR)*, pp. 1874–1883, 2016.
- [18] Olaf Ronneberger, Philipp Fischer, and Thomas Brox, “U-net: Convolutional networks for biomedical image segmentation,” *Proc. of Int. Conf. on Medical Image Computing and Computer-Assisted Intervention (MICCAI)*, pp. 234–241, 2015.

- [19] Diederik P Kingma and Jimmy Ba, “Adam: A method for stochastic optimization,” *arXiv preprint arXiv:1412.6980*, 2014.